JOURNAL OF GEOPHYSICAL RESEARCH, VOL. 87. NO. A4, PAGES 2301-2310, APRIL 1, 1982

FIELD-ALIGNED ION STREAMS IN THE EARTH'S MIDNIGHT REGION

Richard Christopher Olsen
Department of Physics, University of Alabama in Huntsville
Huntsville, Alabama 35899

Abstract. Plasma measurements from the University of California at San Diego auroral particles experiment on the geosynchronous Applied Technology Satellite 6 in the midnight region show that the low-energy ion fluxes (1-100 eV) are field aligned and are well characterized as thermal populations (1-10 eV) with a streaming velocity of 30-100 km/s along the magnetic field line. The lowest energies are found prior to injections, on quiet days, with an increase of the streaming velocity evident when an injection occurs near the satellite. Multiple peaks in the ion distribution functions are attributed to the presence of different ion species (H+, He+, 0+, 0++) streaming at similar velocities, both during quiet times and as the plasma velocity increases in response to an injection.

Introduction

Plasma data from geosynchronous satellites have shown the existence of an extremely variable environment, particularly in the midnight region where the plasma sheet is found, and substorm phenomena are continually observed. Data from the University of California at San Diego (UCSD) auroral particles experiment on Applied Technology Satellite 6 (ATS 6) [Mauk and Mcllwain, 1975] have provided a great deal of information on the magnetospheric plasmas in this region both in the thermal energy range (eV) and in auroral and plasma sheet energy ranges (keV). Lennartsson and Reasoner [1978] and Horwitz and Chappell [1979] studied the nature and the responses to magnetic activity of the warm plasmas. Both studies concentrated on the dayside of the magnetosphere, since the nightside is primarily a region of hot (keV) plasmas. Measurements of low-energy ions on ATS 6 on the nightside are difficult because of generally substantial negative potentials on the spacecraft, and an anticorrelation is observed between such charging events and the presence of warm plasma [Reasoner et al., 1976]. This study generally supports the observations and conclusions of Reasoner et al. [1976] but also indicates that a warm plasma population can be found and analyzed in the midnight region.

Data from ATS 6 were analyzed to determine the characteristics of the thermal plasma prior to and during injection events. Two major characteristics in the nightside thermal plasma were found in the ATS 6 data set:

1. These plasmas are predominantly field aligned.
2. The energy distributions can be fitted by Maxwellian distributions with a bulk velocity parallel to the magnetic fieldline.

The first characteristic, the field alignment of the thermal plasmas, became apparent early in the review of the ATS 6 data. The 10- to 1000-eV ions in the midnight region showed field-aligned pitch angle-distributions throughout the data set. An isotropic background was occasionally present, but the field-aligned fluxes were always dominant. The UCSD detector typically measured down to a pitch angle of 15°, looking from above (north of) the magnetic equator at particles moving towards the pole. The detector rarely measured in the complementary direction, i.e., particles mirroring at the north pole. Measurements down to a few degrees pitch angle were occasionally made, but no indications of an ion loss cone were found or any other suggestions that the field-aligned fluxes might actually be conics. This contrasts with the measurements reported by Horwitz [1980] where dayside and dusk pitch angle distributions frequently showed a conic structure (a peak in flux at pitch angles from 200 to 30°).

Observations of field-aligned beams in other parts of the magnetosphere have been reported by a number of experimenters. S3-3 measurements of ion fluxes in the few-thousand kilometer range reported by Mizera and Fennell [1977] and Shelley et al. [1976], amongst others, established that energetic fluxes of various ion species were being accelerated from the ionosphere into the magnetosphere. GEOS 1 observations at L = 8 using a mass spectrometer show that beams of 20- to 50-eV ions can be found at 1000 LT, with singly charged helium and oxygen present in fair abundance [Young, 1979; Geiss et al., 1978].

ISEE 1 data taken around L = 6 or 7 in the midnight region show a similar result for low-energy (0-50 eV) ions [Baugher et al., 1980, Figure 2d]. Further out, ISEE 1 measurements reported by Sharp et al. [1981] show ion beams in the 0.1- to 1.0-keV energy range in the tail lobes and near the boundary of the plasma sheet. Frank et al. [1977] inferred hydrogen and oxygen beams in the distant tail from doubly peaked distribution functions, as did Hardy et al. [1977]. These latter observations, at lunar orbit, showed thermal (few eV) hydrogen and oxygen streaming along the tail with velocities of the order of 100 km/s. The velocities of the two ion species were similar, rising and falling together during individual measurement periods. There are some indications that this behavior is seen in the ATS 6 plasma sheet measurements, with multiple peaks in the ion distribution function.

The second characteristic of the ATS 6 data set, a field-aligned flow, is clear for hydrogen during some periods of high flow velocity, when there is a distinct peak in the ion distribution function. Plasmas with lower flow energies (less than 5 eV) do not demonstrate this characteristic as clearly, but there are still indications that the plasma is flowing along the field line. In addition to a primary peak in the distribution function attributed to hydrogen, additional peaks or local maxima were frequently observed at higher energies. This effect is interpreted as the result of higher-mass ions streaming along the magnetic field line at velocities similar to the value found for hydrogen.

Paper number 1A1888

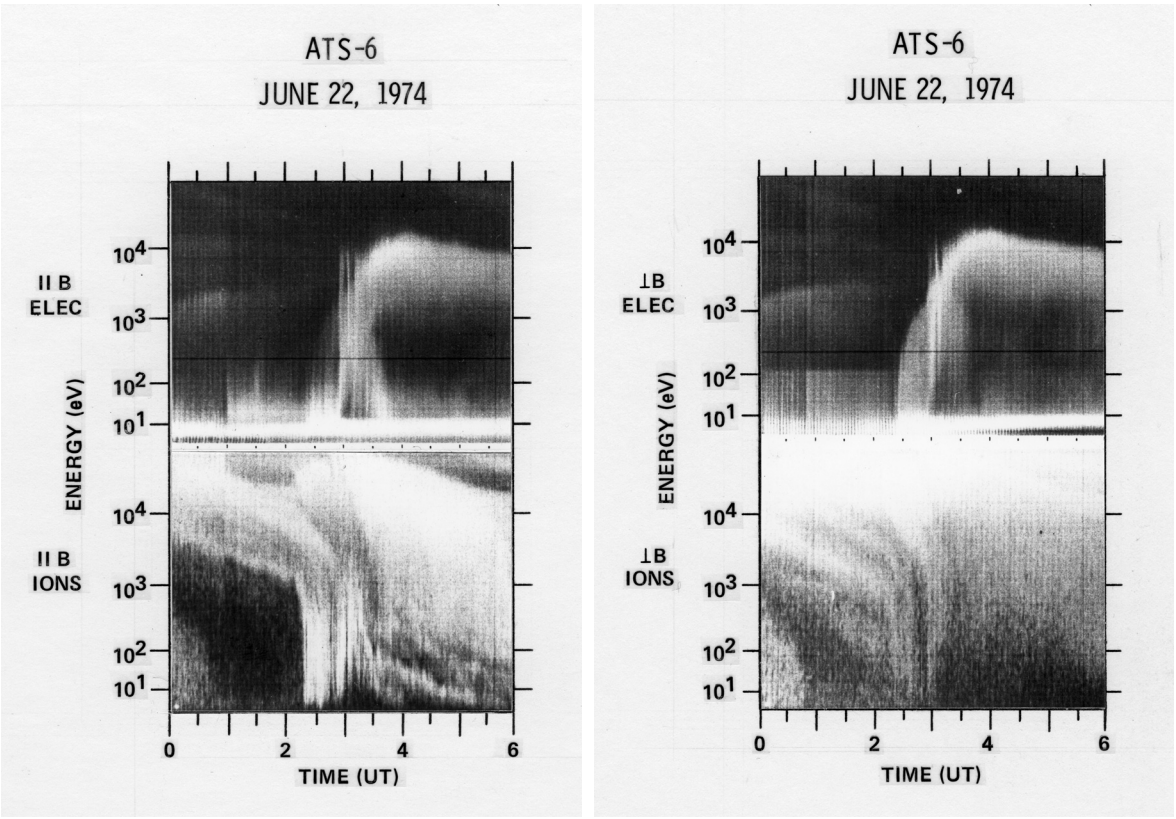

Fig. 1. Spectrograms for June 22, 1974. (a) NS detector parked parallel to the magnetic field line (a 15°). (b) EW detector parked perpendicular to the magnetic field line.

Such an interpretation does not constitute a proof for the existence of multiple ion species, but rather is presented as a likely explanation for the appearance of the data.

The low-energy plasma population near midnight is best studied during relatively quiet times, prior to injections of hot plasma. A practical reason for this, on ATS 6, is that the spacecraft is not generally negatively charged during such times. Also, the intensity of the thermal fluxes at 6.6 RE at midnight seems to increase as magnetic activity decreases. The thermal fluxes generally disappear during active times, though their presence could be masked by the -100- to -1000-V potentials commonly found during such periods. The study of quiet periods tends to restrict the analysis to periods when the spacecraft is near the inner edge of the plasma sheet, but still within that region, rather than in the plasmasphere. This identification of the spacecraft location is based on work by Mcllwain [1972, 1974] and Mauk and Mcllwain [1974] on the ATS 5 data set, establishing the convection patterns for plasmas observed at 6.6 R_E and the injection boundaries where the particles originate. Meng et al. [1979] and Eather et al. [1976] connected the ATS data sets with auroral displays to provide the latitudinal variation (radial at the equator) of the plasma sheet needed to identify the relation-ship of the spacecraft position to the plasma sheet boundary [see Eather et al., 1976, Figure 10a].

Two examples of the ATS 6 observations are presented from the summer and fall of 1974. The first is an encounter with the plasma sheet at 2000 LT, similar to many observed over the lifetime of the detector. The convection pattern of the high-energy ions indicates that for this case the plasma sheet population was formed several hours prior to the satellite's passage. The second event comes on an unusually quiet day, where there is no magnetic activity (i.e., substorms) evident until 0200 LT. The event combines an example of the quiet time characteristics of the thermal plasma with an almost unique example of a steady acceleration of the thermal fluxes at the injection point.

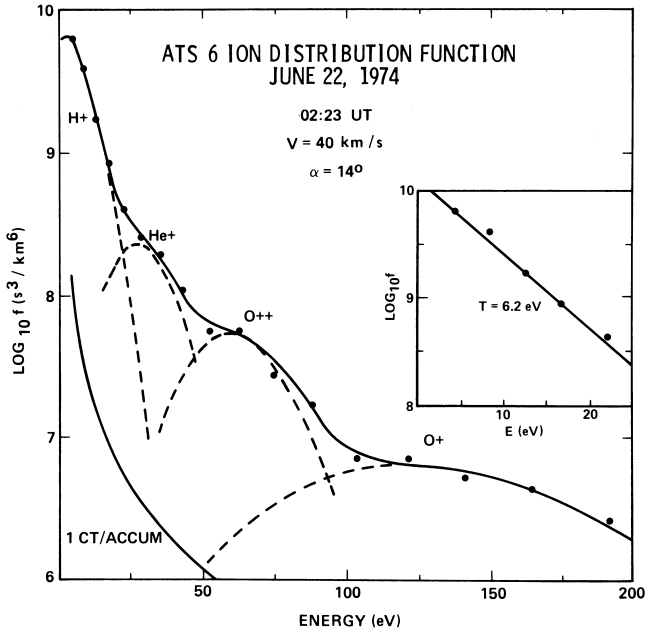

Fig. 2. Ion distribution function, June 22, 1974, 0223 UT. Data are plotted versus E/Q, the measurement parameter. Distribution functions are calculated from count rates assuming a proton mass. Fit parameters are as follows: α = 14°, ϕs/c = +5 V, V = 40 km/s;

	H+	He+	0+	0++
T(eV)	1.55	1.5	8.0	3.5
$4\pi\ \partial n/\partial\Omega$ (cm^{-3})	0.26	0.05	0.02	0.2

Plasma Sheet Entry

The first event is typical of the nightside plasma behavior seen on ATS 6. On this day both rotating heads were fully operational, parked to give the particle fluxes parallel and perpendicular to the magnetic field line. EKp was 14- on the previous day, and the 3-hour Kp values for the beginning of the day were 3, 3, and 1. The data are shown in two spectrograms for the first 6 hours of June 22, 1974. The count rates from the parallel and perpendicular detectors are shown in Figures la and lb, respectively. Black indicates low fluxes, and white, high fluxes as in the low energy electrons (photoelectrons) throughout the day. Both energy axes increase upward, covering the 1-eV to 80-keV energy range of the detectors. The discontinuity at 100 eV in the perpendicular electron data (top half of Figure lb) between 0000 and 0230 UT is due to a change in the detector gain and a change in the background due to secondary electron production.

The spacecraft encounters the plasma sheet boundary at about 0220 UT. This boundary is the zero-energy Alfven layer, or the convection boundary for zero-energy particles. The electron fluxes between 0220 and 0300 UT show the typical signature for such an encounter. They are pancake at higher energies, switching to field aligned below 100 eV. An injection of hot plasma occurs just before 0300, as indicated by the spikes in the keV electron data and the magnetometer data (not shown). This distinction between crossing a spatial boundary (0220) and an injection (0300) is supported by data from ATS 5. ATS 5 was in the same orbit as ATS 6 but trailed by 45 min (11° longitude). ATS 5 did not reach the plasma sheet before the injection but did see the injection within a minute or two of 0300.

Referring to Figures la and 1b, one notes that the ion fluxes seen in the plasma sheet region (0220-0300) below 1 keV are primarily field aligned. Figures 2 and 3 show field-aligned ion distribution functions for the plasma sheet entry period(0223)and the injection period(0259), respectively. A nonflowing Maxwellian distribution function, as is occasionally found in the ion data, would be a straight line on these log-linear plots. The field-aligned fluxes rarely give such a line over the energy range of interest. Nonetheless, in the early stages of analysis, simple Maxwellian fits were tried in the low-energy portions of the distribution function. For example, the 5- to 20-eV portion of the 0223 data can be fitted with parameters n = 3 cm^{-3}, T=6.2 eV, assuming the ions are hydrogen (and $\phi_{s/c}$ = 0). Such fits, however, leave two problems. First, in many of the data sets, a distinct peak was apparent in the distribution function, even when the spacecraft was positive.

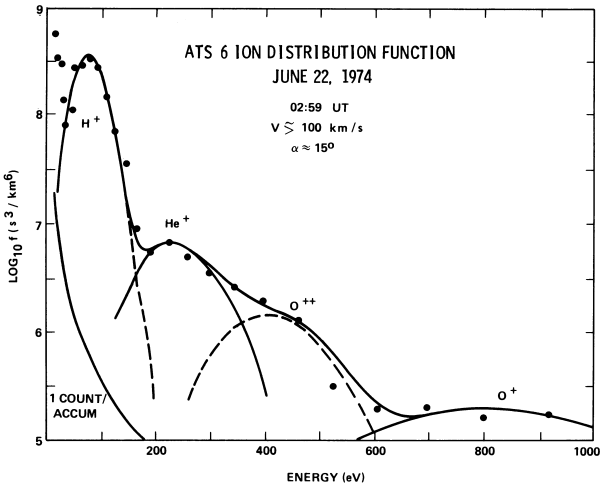

Fig. 3. Ion distribution function, June 22, 1974, 0259 UT. High-velocity streaming is seen here at the time of injection. The three data points from 12 to 22 eV are statistically significant (count rate of 100) and probably represent a background plasma population. Fit parameters are as follows: α = 15°; $\phi_{s/c}$ = +5 V;

	H+	He+	0+	
T(eV)	4	8	32	16
$4\pi\ \partial n/\partial\Omega$ (cm^{-3})	0.16	0.03	0.01	0.2
V(km/s)	125	109	102	102

Even in the 0223 data shown in Figure 2, there is some rounding evident in the first four data points. Second, such fits are inconsistent with the bumps in the distribution function at higher energies that usually occur at integer multiples of the energy of the hydrogen peak, when an Ht peak was apparent, as in the 0259 data in Figure 3. These problems were addressed by fitting the data with a flowing Maxwellian and by assuming a multiple on species composition (H+, He+, 0+, and 0). Thermal energies in the range 1-10 eV and similar velocities (30-100 km/s) were assumed for all ion species. Details of the fitting process are given in an appendix. Briefly, the distribution functions were plotted on an interactive graphics terminal, and the plasma parameters (density, temperature, and flow velocity) were varied to create a fit to the distribution function. It was assumed that the flow was along the magnetic field line, and the pitch angle thus gave the angle between the look direction and flow direction. The spacecraft potential was an additional parameter. The fit was a subjective one and was never quantified with an error estimate, since the number of free parameters occasionally exceeded the number of data points. It is presented as a possible explanation for the appearance of the distribution function at energies above the hydrogen peak.

As applied to the data in Figures 2 and 3, the fit gives plasmas flowing at 40 and 125 km/s, respectively. The 0223 data are typical of pre-injection plasma sheet measurements in this study, with each species assumed to move at equal velocity, typically between 40 and 50 km/s. The hydrogen peak is obscured by the positive spacecraft potential. The injection measurement, at 0259, is typical of such measurements, with a distinct peak attributed to hydrogen and peaks or shoulders at higher energies attributed to other ion species. The high—energy bumps are fitted at slightly different velocities than the hydrogen, reflecting the variation in the ion velocities on a time scale of seconds. The thermal nature of the plasma is more stable up to the injection point, however, with the hydrogen fit increasing only slightly in temperature from 2 to 4 eV. The four lowest—energy data points in Figure 3 (11, 15, 21, and 27 eV) are well above background, with 25—50 counts. These data points may indicate the persistence of the lower—energy plasmas seen before the injection. Following the injection the thermal plasma disappears.

Steady State and Acceleration

The second example shows the thermal plasma behavior observed during very quiet periods and a nearly unique example of a gradual increase in the flow velocity as an injection occurs in the post-midnight region. The single injection, occurring on a quiet day, is the most unique feature of the day. September 18, 1974 (day 261), was a quiet day following an unusually quiet day. September 17 had a ΣKp of 7-, and the 3-hour Kp values for the first 9 hours of the September 18 were 0, 1-, and 2+, the last Kp indicating the resumption of magnetic activity seen by ATS 6 at 0800 UT as an injection.

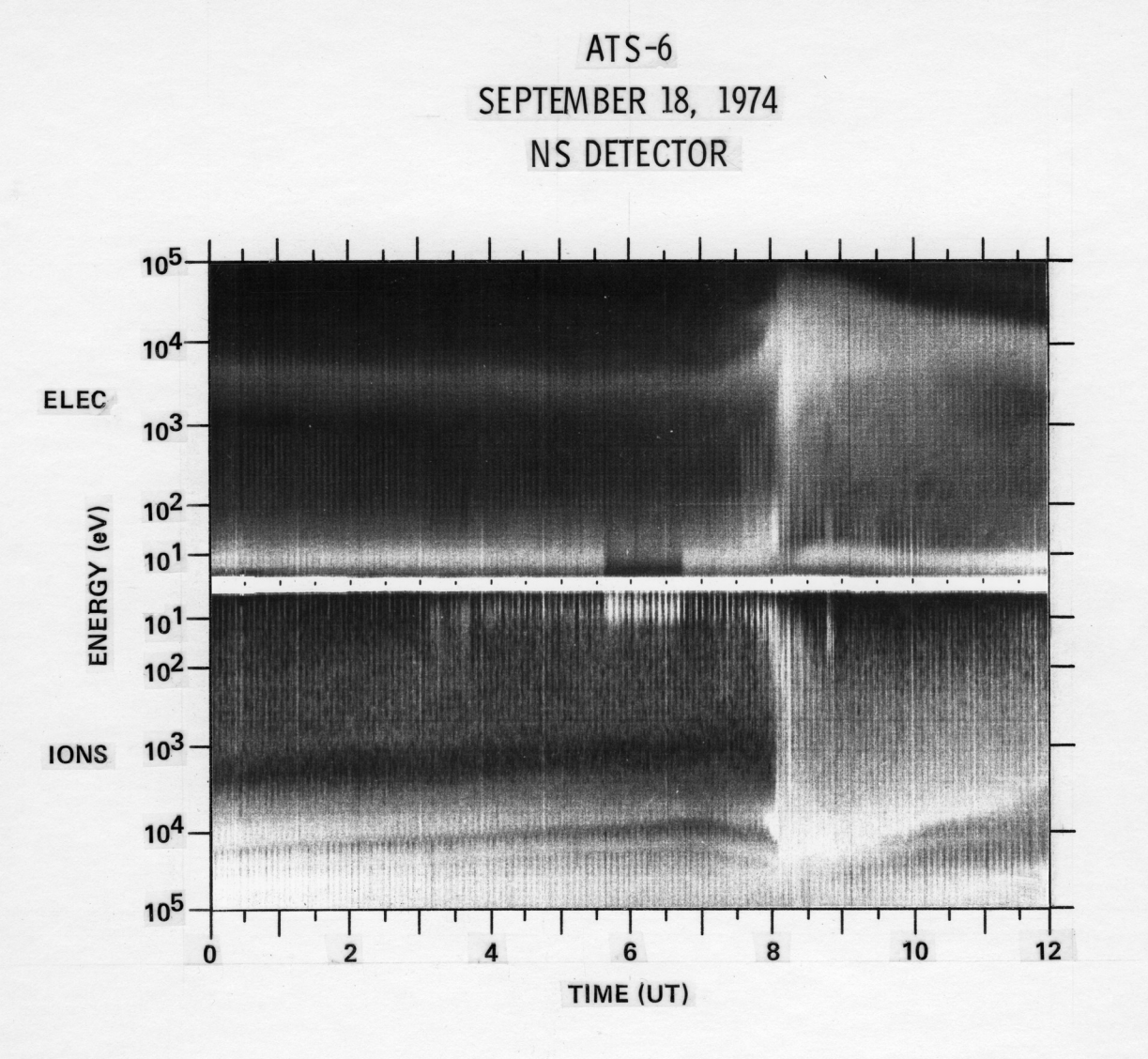

Fig. 4. Spectrogram for September 18, 1974. Data are from the NS rotating detector assembly. An eclipse of the satellite occurs from 0538 to 0642 (determined from solar array telemetry). Vertical striping indicates field-aligned fluxes. An injection of hot plasma occurs at 0800, as shown by the appearance of high fluxes of keV electrons.

A spectrogram (Figure 4) shows the data for the nightside magnetosphere on this day. The arrival of hot plasmas at 0800 is visible in the ion and electron data, as is the field alignment of the ions in the vertical streaking of the spectrogram. The rotating detector samples the field-aligned plasma every 2-3 min. The field alignment is particularly visible in the low-energy ions between 0538 and 0643 UT, when the spacecraft is eclipsed. The absence of photo-electrons at this time allows the spacecraft potential to drop from about +10 V to near zero volts. This significantly improves the ion measurements, since the ion population has a characteristic energy of only 5-10 eV.

The strong field alignment of the ion population during this period is shown in Figure 5, a plot of the pitch angle distribution of the 5-eV ions between 0540 and 0618 UT. The plasma is field aligned within the detectors' ability to measure the distribution, with a half width at half maximum of 20° or less. All of the distribution functions shown for this day were taken at pitch angles less than 20°, usually at 14°-15° pitch angle.

We next show the distribution for the field-aligned ions measured in eclipse, at local midnight, and on into the plasma injection at 0200 LT. Figure 6 shows the distribution function from 0 to 100 eV at 0639, during the eclipse, with a fit to the data based again on the assumption of a flowing Maxwellian, in this case 32 km/s. The part of the distribution function attributed to higher masses forms only a few percent of the flux here.

The 4- to 10-keV electron fluxes begin a gradual increase at about 0730 (see Figure 4), as the injection event approaches.

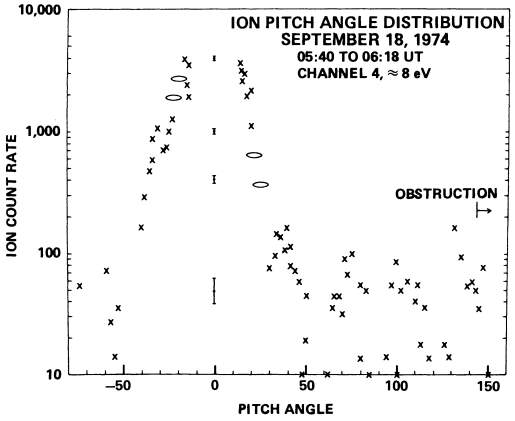

Fig. 5. Pitch angle distribution of low-energy ions, September 18, 1974, 0540-0618 UT. These data were taken during the eclipse of the spacecraft. Pitch angles were determined from magnetic field data from the UCLA magnetometer, courtesy of R. L. McPherron.

Over the next half hour the energy of the thermal plasmas increases, as seen in the increase of the energy of the first peak in the distribution function. The thermal plasma peaks in energy shortly after 0800, Figure 7 shows three spectra from early in the half-hour period, with the fitted velocity increasing from 35 km/s at 0738 to 45 km/s at 0748. Note that the hydrogen temperature remains fairly constant at 2 eV.

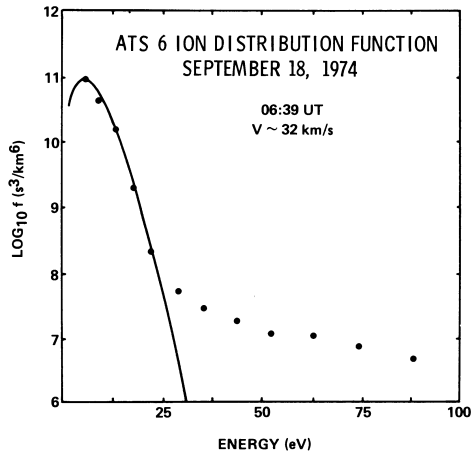

Fig. 6. Ion distribution function, September 18, 1974, 0639 UT, eclipse data. The UCSD detector had been operated for about 100 days by this time, and the spiraltron detectors were showing a significant degradation. The electron detectors seemed to have an even (energy independent) decay, while the ion detectors showed some energy dependence to the decay. Below a few hundred eV, the decay is about a factor of 10 in the ion detectors. This effect has not been included in the calculations. Fit parameters are as follows: α= 14°; $\phi_{s/c}$ = 0 V; V = 32 km/s, T = 1.0 eV; $4\pi\ \partial n/\partial\Omega$ = 1.85 cm^{-3}.

Higher masses become apparent as the streaming velocity increases. Two different fits are shown for the data taken at 0752 UT to illustrate the possibilities for describing the plasma in terms of multiple ion species composition. Figures 8a and 8b show a four-species fit and three-species fit, respectively. Figure 8a shows a 70-km/s fit with hydrogen, singly charged helium, and the two oxygen species. The rounding of the hydrogen peak is apparent at this high velocity. The second peak, at 90 eV, suggests the need for either another hydrogen component or another mass species. The 200- and 400-eV bumps attributed to 0++ and 0+ are less convincing but above statistical fluctuations. The gap between the data and the fit at 50 eV is probably due to a nonthermal character in the hydrogen (here with a 1.3-eV temperature). Figure 8b shows the same sort of fit without the doubly charged oxygen. The fit appears better in places but does not give the similar velocities for all ion species found in Figure 8a. The hydrogen parameters are similar in the two fits, with a temperature of 2 eV in the latter fit, and a streaming velocity of 62 km/s. (The velocity is lower in the second fit because a lower spacecraft potential was assumed.) Helium is close to its prior value of 70 km/s, but the oxygen value is now 38 km/s. This would drop to 33-35 km/s if the 90-eV peak was taken as singly charged oxygen.

The plasma velocity, as obtained from the fitting procedure, varies somewhat between 0750 and 0800, fluctuating about the 50-km/s point, as the injection process approaches completion. Data from 0802 (Figure 9) are well fitted with four ion species flowing at 50 km/s.

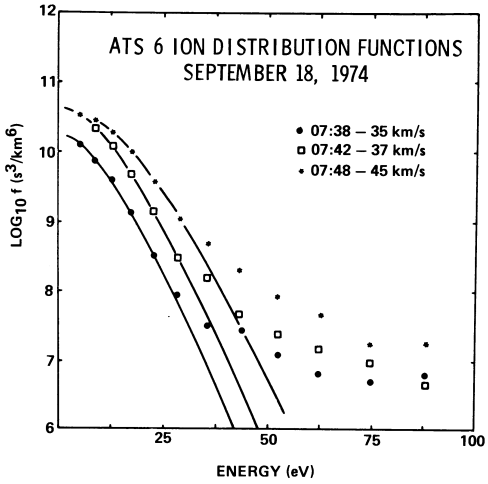

Fig. 7. Ion distribution functions, September 18, 1974. Data from 0738, 0742, and 0748 are given, along with fits, to show the acceleration of the plasma. Data were all taken in sunlight. Hydrogen fit parameters are as follows: $\phi_{s/c}$ = +5 V;

Time	0738	0742	0748
T(eV)	1.8	1.8	2.0
$4\pi\ \partial n/\partial\Omega\ (cm^{-3})$	0.9	2.0	1.8
V(km/s)	35	38	45
α	16	12	12

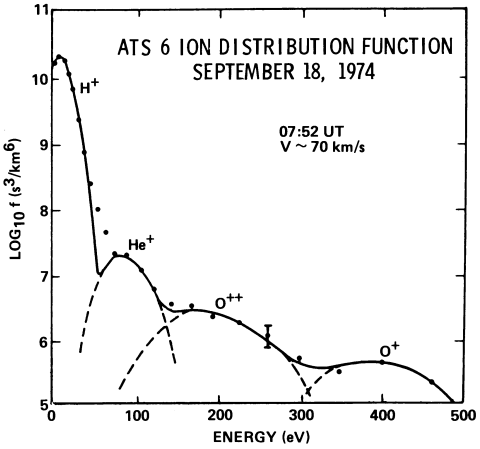

Fig. 8a

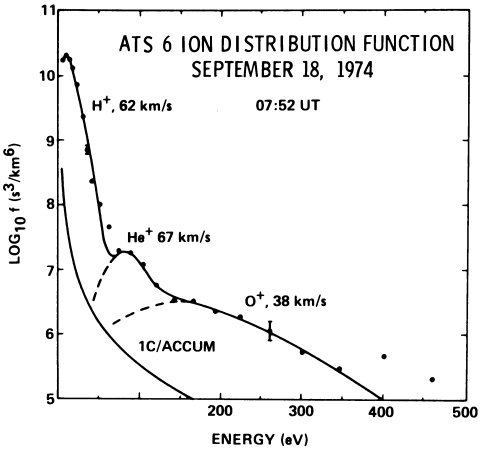

Fig. 8b

Fig. 8. Ion distribution function, September 18, 1974, 0752 UT. Two different versions of the fitting procedure are used on the same data.

(a) Four-species fit. Parameters are as follows: α = 14°; $\phi_{s/c}$ = +14 V; V = 70 km/s;

	H+	He+	0+	0++
T(eV)	1.3	2.6	3.5	12.5
$4\pi\ \partial n/\partial\Omega(cm^{-3})$)	1.0	0.01	0.04	0.03

(b) Three-species fit. Parameters are as follows: α = 14°; $\phi_{s/c}$ = +11 V;

	H+	He+	0+
T(eV)	2.1	1.6	24
$4\pi\ \partial n/\partial\Omega(cm^{-3})$	1.2	0.01	0.04
V(km/s)	62	67	38

This example (with a peak in the distribution function at 12 eV) is the last clear 'thermal' measurement during this time period. Ion fluxes are considerably more energetic after this point, with the field-aligned ions observed with energies up to 10 keV. The ion fluxes are quite variable between 0802 and 0808, but a fairly clear measurement can be made at 0808, as shown in Figure 10. There is a strong peak in the distribution function at 110 eV, which is well modeled by a hydrogen plasma with a temperature of 4 eV, streaming along the field

line at 150-160 km/s. Lesser peaks at higher energies suggest higher masses at velocities of 120-130 km/s. The absence of the thermal (E < 100 eV) ion fluxes persists for an hour or more, which appears to be the typical situation at geosynchronous orbit. The strongly field-aligned fluxes of the plasma sheet seem to consistently accelerate with the appearance of hot plasmas and then disappear in thermal energy ranges (0-100 eV).

Summary

The data shown have demonstrated the normal thermal plasma behavior observed in the midnight region of the magnetosphere. At quiet times, in the absence of particle injections, a low-energy, field-aligned plasma is consistently observed. This 1- to 10-eV plasma is modeled successfully as a Maxwellian with a bulk velocity parallel to the magnetic field line. The flow energy (5 eV) is large compared to the thermal energy (1-2 eV) of the distributions. At the edge of the plasma sheet higher-energy streaming (10-20 eV) is consistently seen, with parallel velocities of 40-50 km/s consistently found at the convection boundary. At injections of hot plasma (substorms), brief periods (minutes) of high-velocity (100-150 km/s) plasma streaming are found. In most of the data sets, local maxima in the distribution functions suggest the possibility of multiple ion species moving at similar velocities. These plasmas consistently disappear after the injection process.

Field-aligned thermal ion distributions such as those presented here would be a natural result of a relatively weak parallel electric field operating at ionospheric altitudes, or slightly higher. Gradual changes in the plasma energy are consistent with variations in low-altitude electric fields during injections.

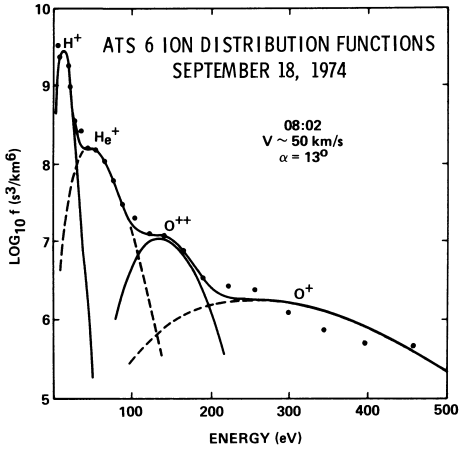

Fig. 9. Ion distribution function, September 18, 1974, 0802 UT. Fit parameters are as follows:

	H+	He+	0+	0++
T(eV)	1.3	4.0	20	6
$4\pi\ \partial n/\partial\Omega(cm^{-3})$	0.11	0.07	0.02	0.1

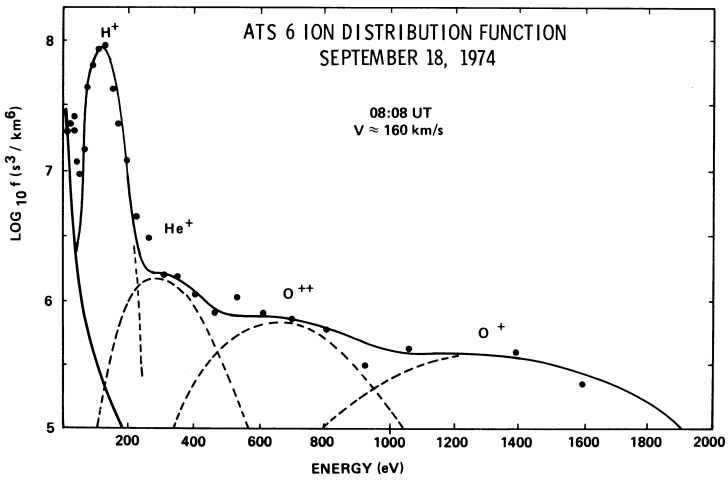

Fig. 10. Ion distribution function, September 18, 1974, 0808 UT. The increasing energy of the plasma is evident in the hydrogen peak, with the plasma velocity between 120 and 160 km/s. The background rate (4 cps) is shown to account for data points below 50 eV. Fit parameters are as follows: $\alpha = 14°$; $\phi_{s/c} = 10$ V;

	H+	He+	0+	0++
T(eV)	4.0	17	47	50
$4\pi\ \partial n/\partial\Omega(cm^{-3})$ (cm-3)	0.07	0.01	0.04	0.07
V(km/s)	157	121	128	128

If such processes are at work, as appears likely from the work of Mizera and Fennell [1977], amongst others, there is the further problem of explaining the similar'velocities of the different ion species inferred here. One attractive possibility is the 'velocity filter' idea discussed by Hardy et al. [1977] in explanation of the hydrogen and oxygen fluxes measured on the lunar surface. Given a limited source size (limited in latitude), a convection electric field, and a reasonable travel distance (a few earth radii), the magnetosphere simply selects ions with similar travel times to reach the satellite together. Since the convection velocity and streaming velocity are mass independent, the filter effect is mass independent. At the L = 7 location of ATS 6, this means that ions streaming up the field line must be convected radially inward to reach the satellite, which is corotating with the source. Higher-velocity fluxes will reach the equator outside the ATS 6 orbit, with lower-energy ions crossing inside the ATS-6 field line. As the convection electric field increases, higher-energy fluxes will reach the satellite, as is observed prior to substorms. The low-energy fluxes seen after long periods of quiet (as in Figure 6) would then be the result of an unusually low dawn-dusk electric field, as well as a weak parallel electric field at the foot of the field line.

This measurement of thermal fluxes at quiet times complements the recently published work by Fennell et al. [1981] and Kaye et al. [1981]. These authors find the plasma sheet to be composed of field-aligned ions below the deep proton minimum [McIlwain, 1972]. Fennell et al. report the field-aligned flux dropping below their detector's sensitivity level or energy range at quiet times, and it can be seen from this study that the 78-eV lower limit of their detector is largely responsible for the observation that the field-aligned fluxes fade with time and that the steady state is below their energy threshold.

The report by Kaye et al. [1981] that the plasma sheet fluxes in the 0.1- to 10-keV energy range showed high 0+/H+ flux ratios (often greater than 1) suggests that the relatively high oxygen content used in some of the fits used here may be reasonable. Preliminary studies of the 0- to 100-eV mass spectrometer data from ISEE 1 by the author show that the plasma sheet population is predominately field aligned, as found here, and that there is a relatively high oxygen flux. In particular, the field-aligned oxygen flux is typically higher than the helium flux, though generally lower than the hydrogen flux in the energy range measured. Doubly charged oxygen is occasionally seen as well, at lower flux levels than the singly charged ions. Doubly charged oxygen was not well sampled in the data set reviewed so far, and it is difficult to say how frequently it appears in the plasma sheet or to estimate the relative flux level.

This analysis of the ATS 6 data suggests that a search for field-aligned fluxes between 1000 and 8000 km should include cases between the 1-eV polar wind energy and 1- to 10-keV auroral energies typically studied at such altitudes. Data from ISEE 1 and DE 1 need to be examined between L = 4 and L 10 for variations in the ion

energy in order to test the velocity filter concept, and future spacecraft and instruments should be designed to look more closely along the magnetic field line, with an angular resolution of a few degrees. The concept of a thermal plasma needs to be expanded to include a 1-eV population at an energy of hundreds of eV, and instruments need to be designed with the necessary energy resolution to measure such a plasma.

Appendix

The fitting procedure used to study the multiply peaked ion distributions was to fit the data to a sum of flowing Maxwellians, with the form

$$f(\vec{v}) = \sum_i n_i \left(\frac{m_i}{2\pi k T_i}\right)^{3/2} \exp -m\left(\frac{(\vec{V}-\vec{V}_i)^2}{2kT_i}\right)$$

where the measured distribution function is corrected for the spacecraft potential. The ion species considered in the analysis were H+, He+, 0+, and 0++. Fitting the data was done on an interactive graphics terminal, varying the parameters until the calculated distribution function agreed with the measured one. This subjective approach was taken because of the relatively high number of variables compared to the number of data points. The objective was not to obtain a 'best' fit, since it was not difficult to fit all the data points exactly, but rather a 'reasonable' fit. Having assumed a form for the plasma distribution (i.e., ions flowing at similar velocities), the point was to determine what sorts of temperatures (and, for H+ and He+, densities) could be inferred.

During the fitting process, low thermal energies (1-10 eV) were assumed initially so that the stream energies could be fitted to the energies of the bumps in the distribution function (usually starting with oxygen, then using that information for the lower masses). Densities and temperatures were then varied to fit the widths and heights of the local peaks. It was assumed that the streams were field aligned, so that the pitch angle could be sued as the angle between the look direction and flow direction. This leaves out the possibility of perpendicular drifts, which are probably small at quiet times but not necessarily so during injections.

This approach introduces a tendency to obtain low temperatures for the hydrogen and helium (i.e., the low-energy part of the curve) instead of higher temperatures and low or zero stream velocities. The density is the most questionable parameter, because all of the other parameters affect it. The strongest effect is in the angle between the look direction and the flow vector, especially for the oxygen. We can see this by evaluating the distribution function at the local maximum which comes at the streaming velocity, or energy (Es):

$$\partial \frac{\log(f(E))}{\partial E} = 0$$

implies $E = E_s \bullet \cos(\theta)^2$

$$f(E) = n\left(\frac{m}{2\pi kT}\right)^{3/2} \exp\left(\frac{-E_s \sin^2(\theta)}{kT}\right)$$

The exponential term can dominate the others which vary in the fitting process. For nominal values of temperature and flow velocity (and the resulting high Mach numbers found for oxygen) it can vary en order of magnitude in a few degrees, thus causing substantial errors in the estimated density.

The count rate can become low enough that statistical fluctuations are a problem, particularly for the oxygen portion of the distribution. Different sets of fit parameters were studied in a number of cases, with one example shown in Figures 8a and 8b. Note the variation in the hydrogen parameters caused by a difference in the assumed potential. The net results of the uncertainties are as follows: (1) Velocity is determined for helium and oxygen within a few percent. Errors in the potential estimate could produce errors in the hydrogen flow velocity of up to 50%, with probable errors of 10%. (2) Temperature is well deter-mined for hydrogen but not well determined for higher masses because of the energy resolution of the instrument. Hydrogen and helium temperatures are determined to within 10% and 50%, respectively, while the oxygen values may have from 100% up to an order of magnitude error. (3) Densities are determined within 10% for hydrogen, 50% for helium, and perhaps an order of magnitude for oxygen.

Acknowledgements. This work was begun while the author was at the University of California at San Diego, under the guidance of C. E. Mcllwain, who provided the data and the equipment necessary to analyze them. The author would like to thank E. Shelley, J. Fennell, and J. Freeman for helpful discussions on the velocity filter concept. This work was supported by NASA/LeRC under NSG-3150, and NASA/MSFC under NAS8-30563.

The Editor thanks D. A. Hardy and J. F. Fennell for their assistance in evaluating this paper.

References

Baugher, C. R., C. R. Chappell, J. L. Horwitz, E. G. Shelley, and D. T. Young, .Initial thermal plasma observations from ISEE-1, Geophys. Res. Lett., 7, 657-660, 1980.

Eather, R. M., S. B. Mende, and R. J. R. Judge, Plasma injection at synchronous orbit and spatial and temporal auroral morphology, J. Geophys. Res., 81, 2805-2824, 1976.

Fennell, J. F., D. R. Croley, and S. M. Kaye, Low-energy ion pitch angle distributions in the outer magnetosphere: Ion zipper distributions, J. Geophys. Res., 86, 3375-3382, 1981.

Frank, L. A., K. L. Ackerson, and D. M. Yeager, Observations of atomic oxygen (0+) in the earth's magnetotail, J. Geophys. Res., 82,129-134, 1977.

Geiss, J., H. Balsiger, P. Eberhardt, H. P. Walker, L. Weber, D. T. Young, and H. Rosenhauer, Dynamics of magnetospheric ion composition as observed by the GEOS mass spectrometer, Space Sci. Rev., 22, 537-566, 1978.

Hardy, D. A., J. W. Freeman, and H. K. Hills, Double-peaked ion spectra in the lobe plasma: Evidence for massive ions?, J. Geophys. Res.,82, 5529-5540, 1977.

Horwitz, J. L., Conical distributions of low-energy ion fluxes at synchronous orbit, J. Geophys. Res., 85, 2057-2064, 1980.

Horwitz, J. L., and C. R. Chappell, Observations of warm plasma in the dayside plasma trough at geosynchronous orbit, J. Geophys. Res., 84, 7075-7090, 1979.

Kaye, S. M., E. G. Shelley, R. D. Sharp, and R. G. Johnson, Ion composition of zipper events, J. Geophys. Res., 86, 3383-3388, 1981.

Lennartsson, W., and D. L. Reasoner, Low-energy plasma observations at synchronous orbit, J. Geophys. Res., 83, 2145-2156, 1978.

Mauk, B. H., and C. E. Mcllwain, Correlation of Kp with the substorm-injected plasma boundary, J. Geophys. Res., 79, 3193-3196, 1974.

Mauk, B. H., and C. E. Mcllwain, ATS-6 auroral particles experiment, IEEE Trans. Aerosp. Electron. Syst., AES-11, 1125-1130, 1975.

Mcllwain, C. E., Plasma convection in the vicinity of the geosynchronous orbit, in Earth's Magnetospheric Processes, edited by B. M. McCormac, pp. 268-279, D. Reidel, Hingham, Mass., 1972.

Mcllwain, C. E., Substorm injection boundaries, in Magnetospheric Physics, edited by B. M. McCormac, pp. 143-154, D. Reidel, Hingham, Mass., 1974.

Meng, C.-I., B. Mauk, and C. E. Mcllwain, Electron precipitation of evening diffuse aurora and its conjugate electron fluxes near the magnetospheric equator, J. Geophys. Res., 84, 2545-2558, 1979.

Mizera, P. F., and J. F. Fennell, Signatures of electric fields and high and low altitude particle distributions, Geophys. Res. Lett., 4, 311-314, 1977.

Reasoner, D. L., W. Lennartsson, and C. R. Chappell, Relationship between ATS-6 spacecraft-charging occurrences and warm plasma encounters, in Spacecraft Charging by Magnetospheric Plasmas, Prog. Astronaut. Aeronaut., vol. 47, edited by A. Rosen, pp 89-101, AIAA, New York, 1976.

Sharp, R. D., D. L. Carr, W. K. Peterson, and E. G. Shelley, Ion streams in the magnetotail, J. Geophys. Res., 86, 4639-4648, 1981.

Shelley, E. G., R. D. Sharp, and R. G. Johnson, Satellite observations of an ionospheric acceleration mechanism, Geophys. Res. Lett., 3, 654-656, 1976.

Young, D. T., Ion composition measurements in magnetospheric modeling, in Quantitative Modeling of Magnetospheric Processes, Geophys. Monogr. Ser., vol. 21, edited by W. P. Olson, AGU, Washington D. C., 1979.

(Received May 7, 1981;
revised December 11, 1981;
accepted December 14, 1981.)